

Electron calorimetry and the e/π ratio in the MINERvA test beam.

William Bergan

January 24, 2015

Abstract

We instituted a number of cuts to isolate a sample of electrons with momenta between 400 and 500 MeV from the pion background and clean out bad events. These cuts had an efficiency of 64% and a pion rejection rate of 91% in the ECAL-HCAL. In our region of interest, we estimate of pion background to be under 1%. We computed MC/data ratios to be 0.996 ± 0.017 statistical ± 0.038 systematic for positive pions, 1.017 ± 0.016 statistical ± 0.041 systematic for negative pions, and 0.969 ± 0.017 statistical ± 0.032 systematic for electrons. We computed the e/π ratios for low-momentum electrons and pions, with the electrons having momenta between 400 and 500 MeV/c and the pions having momenta between 450 and 550 MeV/c. We took the ratio of this for MC over data, finding values of 0.953 ± 0.022 statistical ± 0.021 systematic for the negative pions and 0.973 ± 0.023 statistical ± 0.020 systematic for positive pions in the ECAL/HCAL.

1 To-Do

I will later include tables of the cut efficiencies for my electron selection. I have updated all the tables, and added some new ones, correcting for cross-talk by subtracting 4.2% from the measured energy. I will change the systematic error dealing with cross-talk to reflect this. I have corrected for pileup by subtracting 4 MeV from each event. I have also included histograms showing electron response fractions, both for data and MC, as well as the MC which was cut out by either the electrons selection cuts or cleanliness cuts. (These plots were done before applying the cross-talk correction, but that is just an overall factor, so any analysis comparing the plots should still be accurate.) I have since removed the one bad event in EH data with a visible energy 1.4 times the beamline energy, since it looks like two particles are in the detector. The tables have been updated. I have included a summary table at the end.

2 Introduction

In order to better understand the MINERvA electromagnetic response at higher energies than we are able to study using Michel electrons, we are studying electron/positron¹ events in the testbeam detector. In the lower left corner of Fig. 1, there is a small electron sample with momenta below 500 MeV and time of flight less than 20.5 ns which is separate from the pions. We will then focus our attention on electrons in that region, where the pion background is relatively low. We will use a 400 MeV floor, since we are not sure that we understand what is happening at lower momenta.

Hadronic energy is harder to simulate than electromagnetic energy. However, we are able to use ratios between the electron and pion energy responses in the detector in data and Monte Carlo to test the modeling of the pion response with reduced errors since, by using a ratio, we are able to cancel many of the shared errors. In the remainder of this paper, we will detail our methods for the selection of the electron and pion events, then will compute the e/π ratios and the associated systematic errors.

3 Selection of Events

We restricted ourselves to using only events which had `mtest_pass_all > 0` (to select only events which have an associated reconstructed momentum and reasonable values for their other measurements) and only one

¹In the future, I will use “electron” to refer to both electrons and positrons.

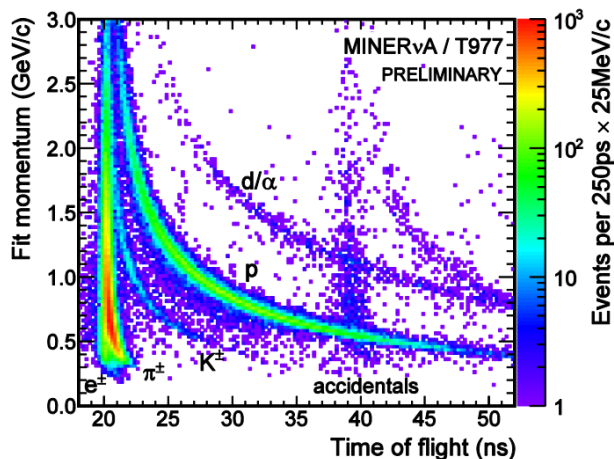


Figure 1: Histogram of momentum and time of flight of particles in beamline. The electron-rich region is in the bottom left corner, with momentum less than 500 MeV/c and TOF less than 20.5 ns. (Taken from Josh Devan - docdb 5920.)

reconstructed track ($n_{\text{tracks}} = 1$), since we did not want to have a second particle contaminating our results. We designed a series of electron cuts to pick out the electrons from the pion background, which we will discuss later. Pions were identified by requiring that they be tagged as a pion ($\text{mtest_pdg} = -211$ or 211) and that they had a reconstructed mass within 100 MeV of the true pion mass. We noticed that we still had events with extra particles in them, so we required all particles to pass a custom cleanliness cut, discussed below. We selected our electrons to be in the electron-rich region with momenta between 400 and 500 MeV, but had the pions in Rik's pion bin at 450-550 MeV momentum to match what Rik Gran had studied, and which we believe we understand reasonably well.

4 Electron Cuts

To get a clean electron sample, we required that they be classified with mtest_pdg equal to ± 11 . I also instituted a series of cuts which are described below to weed out any remaining pions. After applying these cuts and the cleanliness cuts mentioned below, except for the time-of-flight and pdg identification ones², we found that, for particles with momenta between 400 and 500 MeV, 5% of pions and 61% of electrons passed in the TE Monte Carlo and 8% of pions and 73% of electrons passed in the EH MC. As a check, we made histograms of all particles in ECAL-HCAL data which passed the electron cuts, except the time-of-flight and particle-ID ones, as a function of time of flight. We could see a pion and electron peak and, by fitting the pion peak to a Gaussian, could estimate the background in the electron sample. These plots are shown as Fig. 3 and Fig. 2. Unless noted otherwise, all plots shown in this section are for electrons or pions with momenta between 400 and 500 MeV.

4.1 Track Node Cut

We guessed that the number of track nodes would be lower for electrons, since they would typically travel a shorter distance in the detector. Upon examination of the appropriate histograms, shown as Fig. 4 - 7, we required that the number of track nodes be less than 33 in the Tracker-ECAL and less than 20 in the ECAL-HCAL.

4.2 Back-Half Energy

We assumed that pions would penetrate the back-half of the detector more than electrons, so we decided to make a cut based on the fraction of the energy in the back half of the detector. After looking at the Monte

²We left these out since they only appeared in the Monte Carlo as the truth values, and would give us a 100% pion rejection.

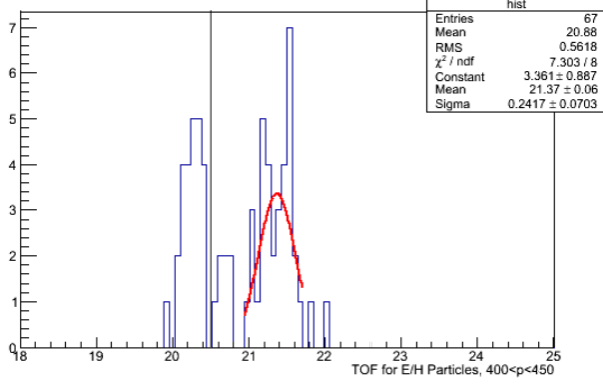


Figure 2: Fitting a Gaussian to the pion peak in the time-of-flight histogram, we estimate 0.01 pions in the 25 electron events with momenta between 400 and 450 MeV.

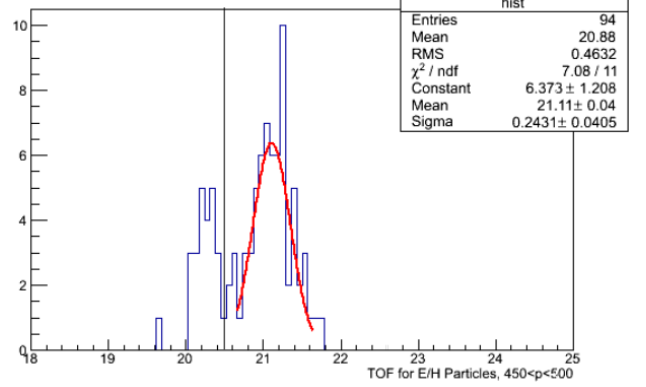


Figure 3: Fitting a Gaussian to the pion peak in the time-of-flight histogram, we estimate 0.3 pions in the 25 electron events with momenta between 450 and 500 MeV.

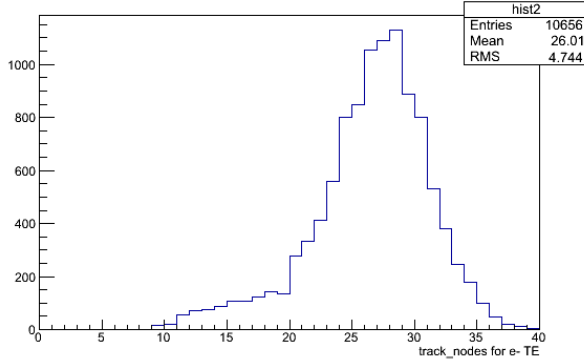


Figure 4: Number of track nodes for electrons in the Tracker-ECAL.

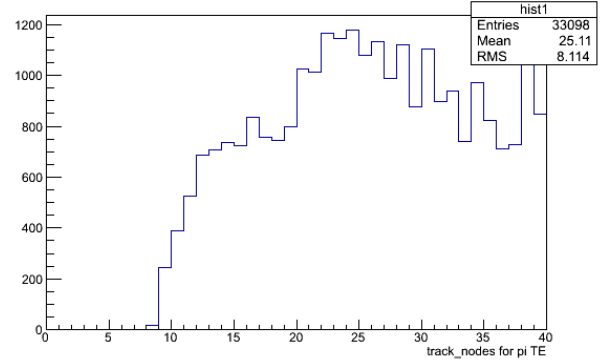


Figure 5: Number of track nodes for pions in the Tracker-ECAL.

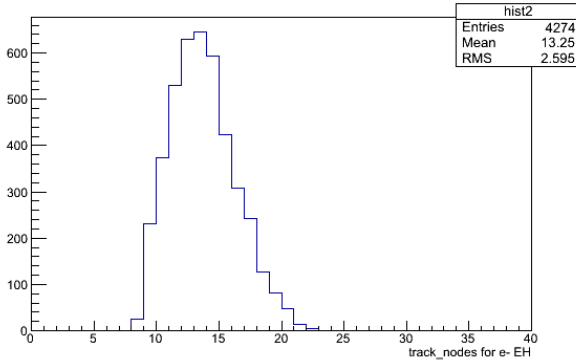


Figure 6: Number of track nodes for electrons in the ECAL-HCAL.

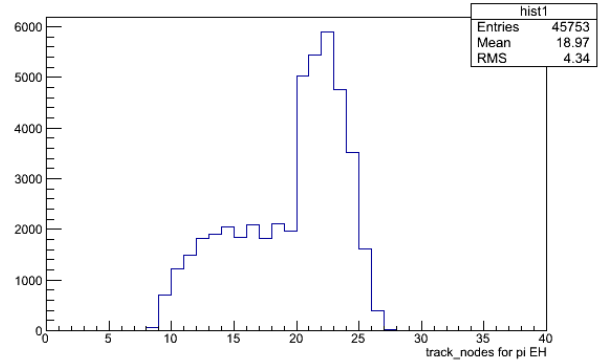


Figure 7: Number of track nodes for pions in the ECAL-HCAL.

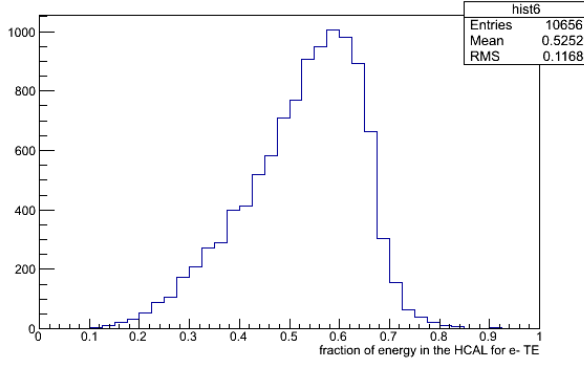


Figure 8: Fraction of the energy in the ECAL for electrons in the Tracker-ECAL.

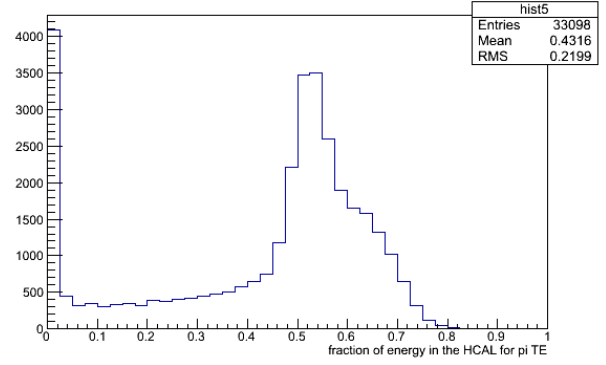


Figure 9: Fraction of the energy in the ECAL for pions in the Tracker-ECAL.

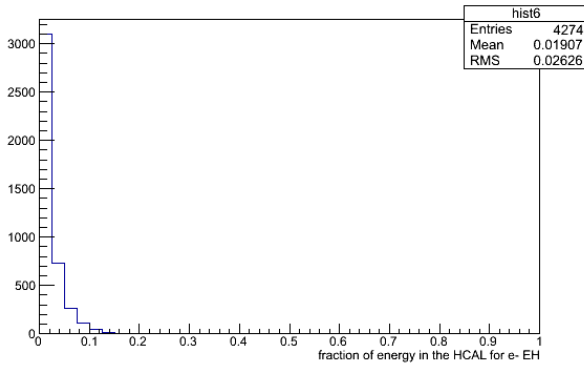


Figure 10: Fraction of the energy in the HCAL for electrons in the ECAL-HCAL.

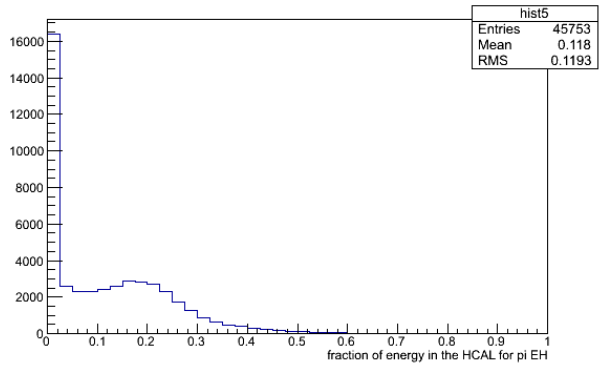


Figure 11: Fraction of the energy in the HCAL for pions in the ECAL-HCAL.

Carlo, we realized that this was only true in the ECAL-HCAL, but, in the Tracker-ECAL, the electrons had more energy in the back half of the detector. We then required that greater than 20% of the visible energy is in the ECAL in the Tracker-ECAL and that less than 10% of the energy is in the HCAL in the ECAL-HCAL. These values are taken before applying the calorimetric corrections. See Fig. 8 - 11.

4.3 Module Variance

Since pions generally travel through the detector in a MIP-like fashion, we expect them to deposit roughly the same energy in each plane, while an electron will have much greater variation. We therefore decided to institute a cut based on the variance in the energy in each of the 40 planes in the testbeam detector. We compute the module variance by finding the visible energy in each module (before calorimetric corrections) and computing the variance in those values. We required that this variance be between 250 and 1550 in the Tracker-ECAL and over 500 in the ECAL-HCAL. See Fig. 12 - 15.

4.4 Number of Raw Hits

We assumed that electrons and pions would generate different numbers of hits (`n_rawhits`) in the detector. After looking at the Monte Carlo histograms, shown as Fig. 16 - 19, we required that `n_rawhits` be over 150 in the Tracker-ECAL and over 110 in ECAL-HCAL.

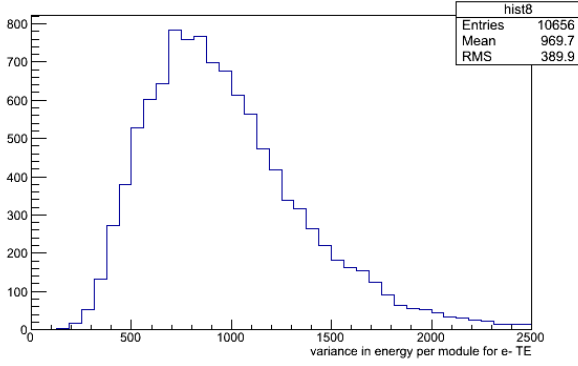


Figure 12: Variance in the energy per module for electrons in the Tracker-ECAL.

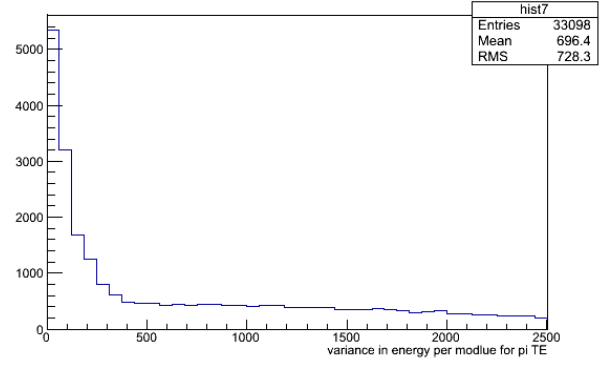


Figure 13: Variance in the energy per module for pions in the Tracker-ECAL.

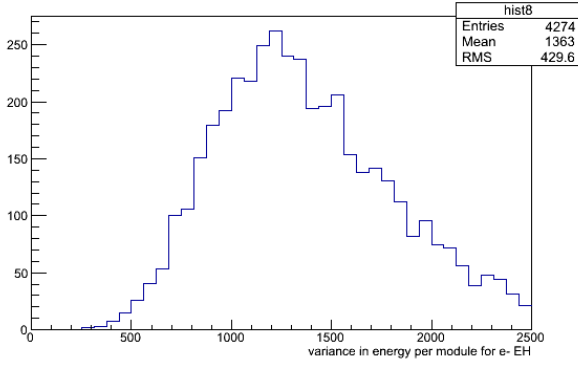


Figure 14: Variance in the energy per module for electrons in the ECAL-HCAL.

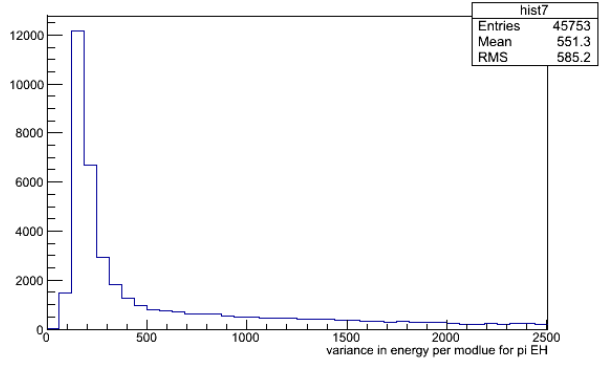


Figure 15: Variance in the energy per module for pions in the ECAL-HCAL.

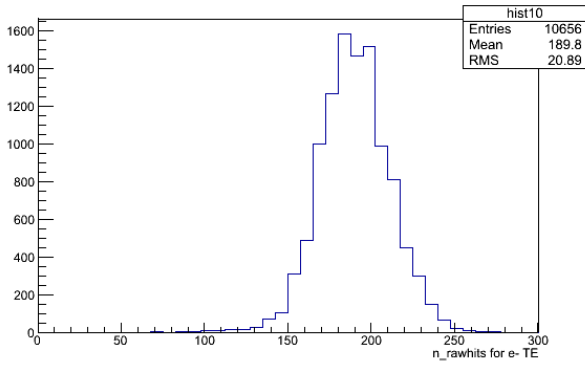


Figure 16: Number of raw hits for electrons in the Tracker-ECAL.

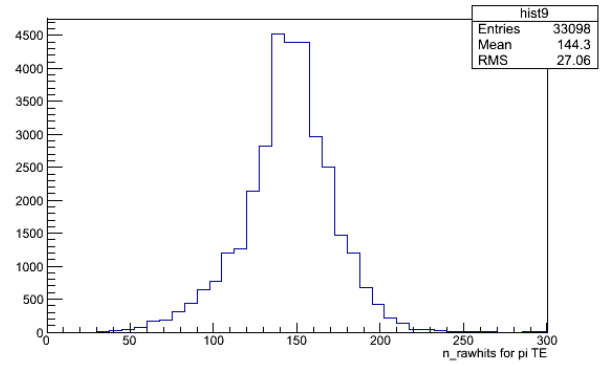


Figure 17: Number of raw hits for pions in the Tracker-ECAL.

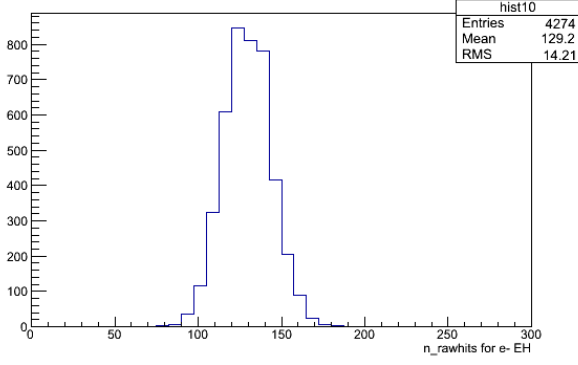


Figure 18: Number of raw hits for electrons in the ECAL-HCAL.

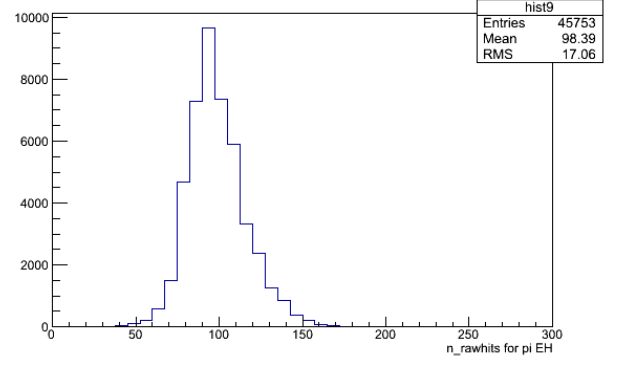


Figure 19: Number of raw hits for pions in the ECAL-HCAL.

4.5 Time of Flight

In order to ensure that we are working in the electron-rich region with a minimal pion background, we require that the time of flight be less than 20.5 ns. See Fig. 1.

5 Cleanliness Cuts

In addition, we introduced a cleanliness cut to remove events containing multiple particles which were not caught by the selection criteria described above. We compute the energy-weighted variance in the hit strip for hits with over 1 MeV of energy in the first two x planes and require it to be less than one.: We require that all events have all their hits roughly in-time and near the track. We focused on the x planes, as we could easily compare strip numbers between them. We computed an energy weighted mean-hit-strip and required that all hits in an event be within 30 strips of it. We also took the energy-weighted mean of the time of all hits within 5 strips of the mean strip and required that no hit be more than 50 ns before this mean time unless it was itself within 5 strips of the mean strip. These choices were based on the plots shown as Fig. 20 - Fig. 31. Removing this cleanliness cut results in the MC/data ratios decreasing by 2.7% for electrons, 12% for negative pions, and 9% for positive pions, indicating an increase in data relative to Monte Carlo. (This has not been updated from the old runs, but the principle should be the same). This is consistent with the cleanliness cut's hoped-for goal of removing events contaminated by extra particles. (The plots right now are for 400-500 MeV pions. I will generate a new round of plots leaving out the strip_var cut, and also combine the different particles into one plot.) See also docdb 9404 and 9441.

6 Visible vs True Energy Response

For each event, we recorded the visible energy as the sum of the energy in all hits in the detector multiplied by the calorimetric constants from Rik's technote (docdb 9474). The true energy was taken from the relativistic formula $E = \sqrt{p^2 + m^2}$, where the momentum is the momentum measured by the beamline and the mass is either 0.511 MeV/c² or 139.57018 MeV/c², depending on whether the particle in question is believed to be an electron or a pion. For each event, we divided the visible energy by the true energy to get the fraction of the energy reconstructed and took the average of these for each particle type (electrons and positive and negative pions) to get the average energy response for that particle. We divided the response in the Monte Carlo by the response in data to get the MC/data ratio for each particle, then divided the electron response by the positive and negative pion responses to get the e/π double ratios. These are quoted in Tab. 1 for the ECAL/HCAL. This also includes the same ratios using pions in the 400-500 MeV range, consistent with the electrons. There is not a large difference between the results from using the two methods. The values we obtain for the MC/data calorimetric response ratio for the 450-550 MeV pions agree well with what Rik found, detailed in docdb 9474, and are consistent with unity. However, the data and MC values themselves

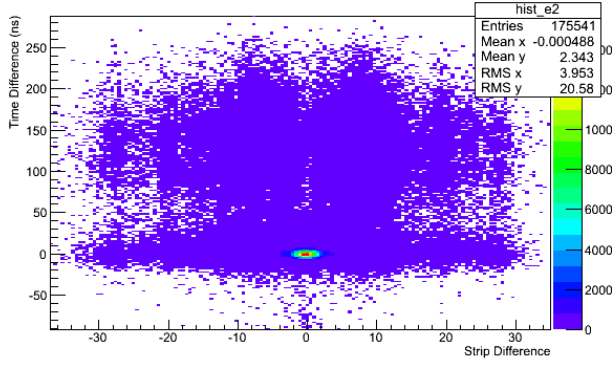


Figure 20: Energy-weighted histogram of hits showing their distance from the main part of the track and their difference in time from the mean time of hits in the track for electrons in EH MC.

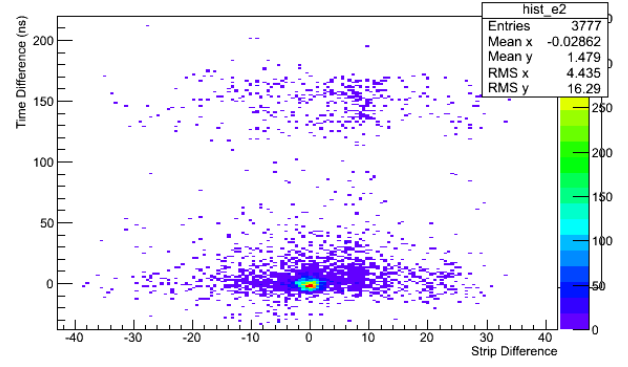


Figure 21: Energy-weighted histogram of hits showing their distance from the main part of the track and their difference in time from the mean time of hits in the track for electrons in EH data.

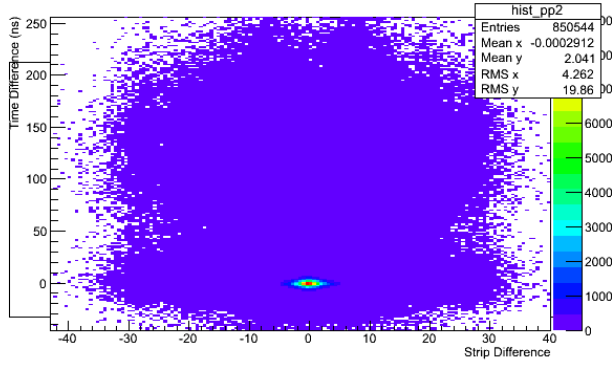


Figure 22: Energy-weighted histogram of hits showing their distance from the main part of the track and their difference in time from the mean time of hits in the track for positive pions in EH MC.

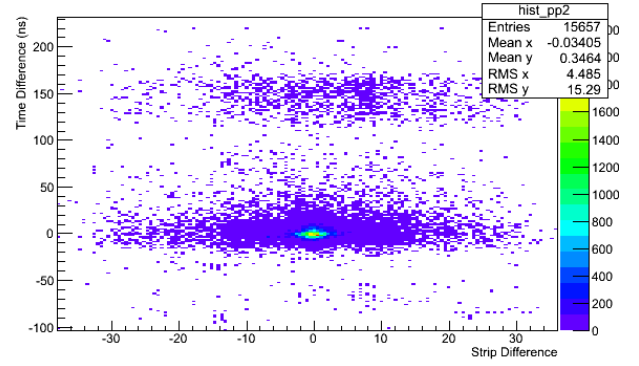


Figure 23: Energy-weighted histogram of hits showing their distance from the main part of the track and their difference in time from the mean time of hits in the track for positive pions in EH data.

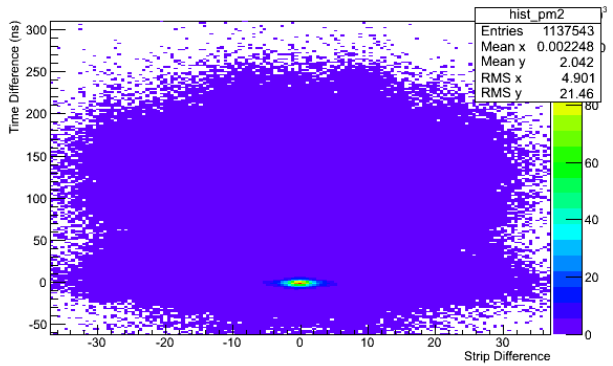


Figure 24: Energy-weighted histogram of hits showing their distance from the main part of the track and their difference in time from the mean time of hits in the track for negative pions in EH MC.

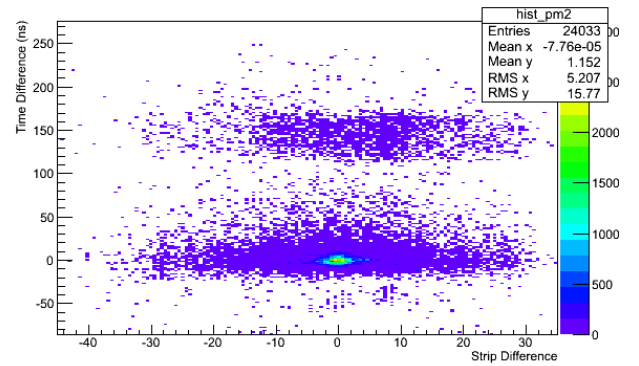


Figure 25: Energy-weighted histogram of hits showing their distance from the main part of the track and their difference in time from the mean time of hits in the track for negative pions in EH data.

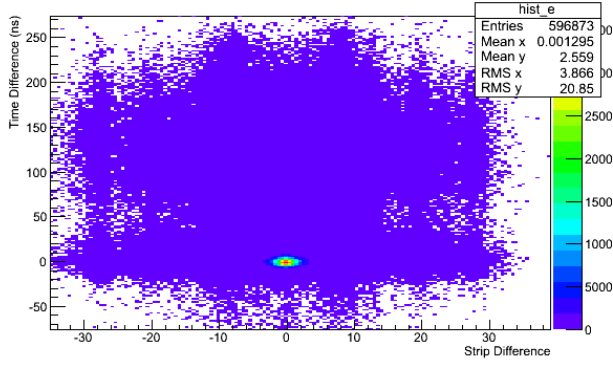


Figure 26: Energy-weighted histogram of hits showing their distance from the main part of the track and their difference in time from the mean time of hits in the track for electrons in TE MC.

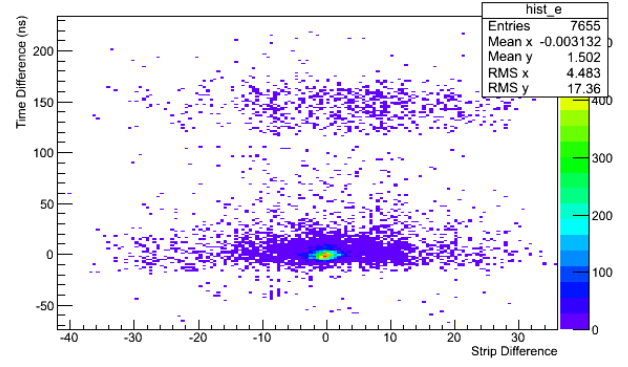


Figure 27: Energy-weighted histogram of hits showing their distance from the main part of the track and their difference in time from the mean time of hits in the track for electrons in TE data.

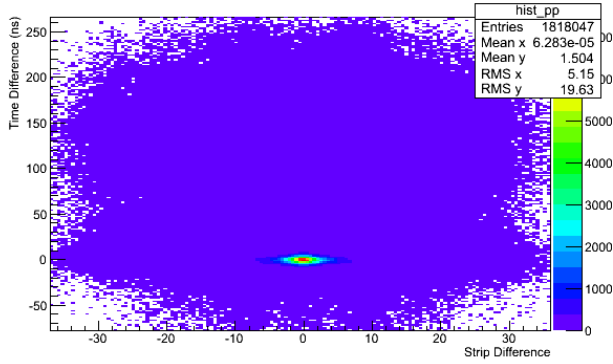


Figure 28: Energy-weighted histogram of hits showing their distance from the main part of the track and their difference in time from the mean time of hits in the track for positive pions in TE MC.

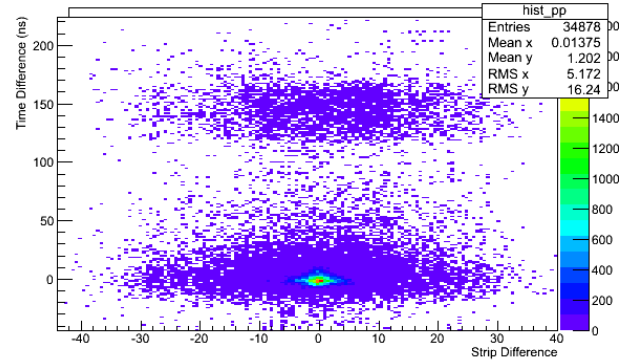


Figure 29: Energy-weighted histogram of hits showing their distance from the main part of the track and their difference in time from the mean time of hits in the track for positive pions in TE data.

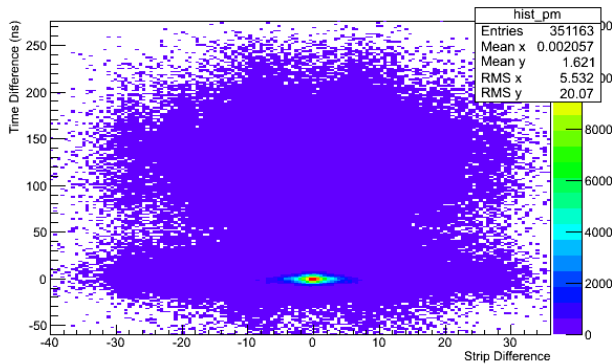


Figure 30: Energy-weighted histogram of hits showing their distance from the main part of the track and their difference in time from the mean time of hits in the track for negative pions in TE MC.

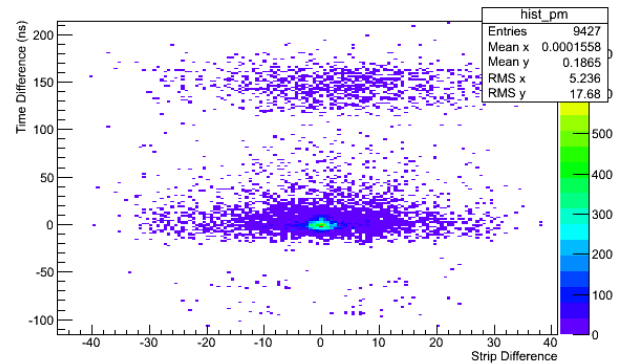


Figure 31: Energy-weighted histogram of hits showing their distance from the main part of the track and their difference in time from the mean time of hits in the track for negative pions in TE data.

EH Full Ratios

Particle	Fraction of Energy Visible in MC	Fraction of Energy Visible in Data	MC/Data
e	0.740 ± 0.002	0.763 ± 0.013	0.969 ± 0.017
π^- 400-500 MeV	0.625 ± 0.002	0.607 ± 0.011	1.030 ± 0.019
π^+ 400-500 MeV	0.626 ± 0.002	0.624 ± 0.011	1.003 ± 0.018
π^- 450-550 MeV	0.635 ± 0.002	0.624 ± 0.010	1.017 ± 0.016
π^+ 450-550 MeV	0.646 ± 0.002	0.649 ± 0.011	0.996 ± 0.017
e/π^- 400-500 MeV	1.182 ± 0.005	1.257 ± 0.031	0.940 ± 0.024
e/π^+ 400-500 MeV	1.182 ± 0.005	1.224 ± 0.030	0.965 ± 0.024
e/π^- 450-550 MeV	1.165 ± 0.004	1.222 ± 0.028	0.953 ± 0.022
e/π^+ 450-550 MeV	1.144 ± 0.004	1.176 ± 0.028	0.973 ± 0.023

Table 1: The e, π , and e/π reconstructed energy fractions for both the 400-500 and 450-550 pions in ECAL/HCAL. All electrons are taken in the 400-500 MeV momentum range. The errors quoted are purely statistical.

TE Full Ratios

Particle	Fraction of Energy Visible in MC	Fraction of Energy Visible in Data	MC/Data
e	0.761 ± 0.001	0.785 ± 0.009	0.969 ± 0.011
π^- 400-500 MeV	0.482 ± 0.002	0.516 ± 0.013	0.934 ± 0.024
π^+ 400-500 MeV	0.534 ± 0.001	0.544 ± 0.007	0.981 ± 0.013
π^- 450-550 MeV	0.462 ± 0.002	0.484 ± 0.011	0.955 ± 0.023
π^+ 450-550 MeV	0.509 ± 0.001	0.527 ± 0.006	0.966 ± 0.012
e/π^- 400-500 MeV	1.578 ± 0.008	1.520 ± 0.042	1.038 ± 0.029
e/π^+ 400-500 MeV	1.425 ± 0.004	1.442 ± 0.026	0.988 ± 0.018
e/π^- 450-550 MeV	1.645 ± 0.007	1.621 ± 0.043	1.015 ± 0.027
e/π^+ 450-550 MeV	1.493 ± 0.004	1.488 ± 0.025	1.004 ± 0.017

Table 2: The e, π , and e/π reconstructed energy fractions for both the 400-500 and 450-550 pions in TRAK/ECAL. All electrons are taken in the 400-500 MeV momentum range. The errors quoted are purely statistical.

are a few percent larger than Rik's values. We have also included plots of how the energy response changes with momentum, which may be seen as Fig. 38 - 41.

We also looked at 50 MeV bin momentum intervals to see how the responses changed. We noticed that there was a distinct change in electron behavior at 450 MeV, with higher-momentum electrons having a greater calorimetric response in the Monte Carlo without a corresponding change in the EH Monte Carlo. See Tab. 3 - 7 More details may be found in docdb 9865.

7 Systematics

We investigated the effects of a number of systematic variations. The results are summarized below in Tab. 9. Similar information is present in docdb 9865.

7.1 Late Energy

Based on the systematics listed in Rik's note, we cut events with over 1 MeV of energy in the last 4 planes (before applying calorimetric corrections).

7.2 Crosstalk

Based on Rik's systematics, we did not count hits with less than half an MeV (before calorimetric corrections).

EH Calorimetric Ratios in the 400-450 MeV Momentum Range

Particle	Fraction of Energy Visible in MC	Fraction of Energy Visible in Data	MC/Data
e	0.744 ± 0.003	0.736 ± 0.014	1.011 ± 0.019
π^-	0.618 ± 0.003	0.600 ± 0.018	1.031 ± 0.032
π^+	0.612 ± 0.003	0.609 ± 0.016	1.004 ± 0.027
e/π^-	1.203 ± 0.007	1.227 ± 0.044	0.981 ± 0.035
e/π^+	1.217 ± 0.007	1.208 ± 0.039	1.007 ± 0.033

Table 3: The e, π , and e/π reconstructed energy fractions for electrons and pions in the 400-450 MeV momentum interval in ECAL/HCAL.

TE Calorimetric Ratios in the 400-450 MeV Momentum Range

Particle	Fraction of Energy Visible in MC	Fraction of Energy Visible in Data	MC/Data
e	0.767 ± 0.001	0.801 ± 0.014	0.958 ± 0.016
π^-	0.497 ± 0.004	0.532 ± 0.022	0.934 ± 0.040
π^+	0.546 ± 0.002	0.572 ± 0.012	0.954 ± 0.020
e/π^-	1.543 ± 0.013	1.505 ± 0.068	1.025 ± 0.047
e/π^+	1.406 ± 0.005	1.401 ± 0.037	1.003 ± 0.027

Table 4: The e, π , and e/π reconstructed energy fractions for electrons and pions in the 400-450 MeV momentum interval in TRAK/ECAL.

EH Calorimetric Ratios in the 450-500 MeV Momentum Range

Particle	Fraction of Energy Visible in MC	Fraction of Energy Visible in Data	MC/Data
e	0.736 ± 0.002	0.792 ± 0.021	0.929 ± 0.024
π^-	0.630 ± 0.002	0.612 ± 0.014	1.029 ± 0.024
π^+	0.635 ± 0.003	0.632 ± 0.014	1.005 ± 0.023
e/π^-	1.168 ± 0.006	1.294 ± 0.045	0.903 ± 0.032
e/π^+	1.159 ± 0.006	1.253 ± 0.043	0.925 ± 0.032

Table 5: The e, π , and e/π reconstructed energy fractions for electrons and pions in the 450-500 MeV momentum interval in ECAL/HCAL.

TE Calorimetric Ratios in the 450-500 MeV Momentum Range

Particle	Fraction of Energy Visible in MC	Fraction of Energy Visible in Data	MC/Data
e	0.754 ± 0.002	0.771 ± 0.012	0.978 ± 0.015
π^-	0.474 ± 0.003	0.506 ± 0.015	0.937 ± 0.029
π^+	0.526 ± 0.001	0.528 ± 0.009	0.995 ± 0.018
e/π^-	1.589 ± 0.010	1.523 ± 0.052	1.043 ± 0.036
e/π^+	1.434 ± 0.005	1.459 ± 0.034	0.983 ± 0.023

Table 6: The e, π , and e/π reconstructed energy fractions for electrons and pions in the 450-500 MeV momentum interval in TRAK/ECAL.

EH Calorimetric Ratios in the 500-550 MeV Momentum Range

Particle	Fraction of Energy Visible in MC	Fraction of Energy Visible in Data	MC/Data
e	0.734 ± 0.002	0.808 ± 0.026	0.908 ± 0.029
π^-	0.638 ± 0.002	0.634 ± 0.013	1.008 ± 0.021
π^+	0.655 ± 0.002	0.662 ± 0.015	0.991 ± 0.023
e/π^-	1.149 ± 0.005	1.276 ± 0.049	0.901 ± 0.035
e/π^+	1.119 ± 0.005	1.222 ± 0.048	0.916 ± 0.037

 Table 7: The e, π , and e/π reconstructed energy fractions for electrons and pions in the 500-550 MeV momentum interval in ECAL/HCAL.

TE Calorimetric Ratios in the 500-550 MeV Momentum Range

Particle	Fraction of Energy Visible in MC	Fraction of Energy Visible in Data	MC/Data
e	0.738 ± 0.002	0.769 ± 0.017	0.960 ± 0.021
π^-	0.451 ± 0.003	0.466 ± 0.016	0.969 ± 0.035
π^+	0.496 ± 0.001	0.527 ± 0.008	0.942 ± 0.015
e/π^-	1.636 ± 0.010	1.651 ± 0.068	0.991 ± 0.042
e/π^+	1.489 ± 0.005	1.460 ± 0.040	1.020 ± 0.028

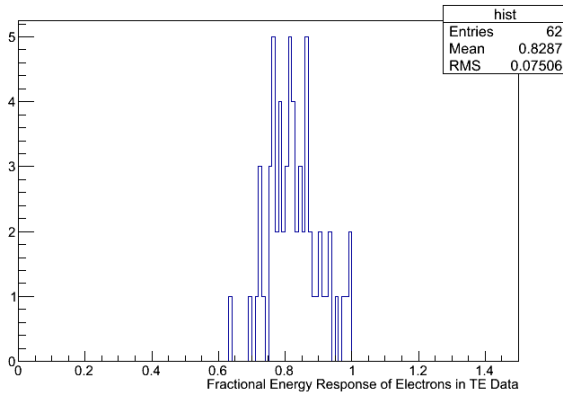
 Table 8: The e, π , and e/π reconstructed energy fractions for electrons and pions in the 500-550 MeV momentum interval in TRAK/ECAL.


Figure 32: Histogram of electron calorimetric response for Tracker-ECAL data.

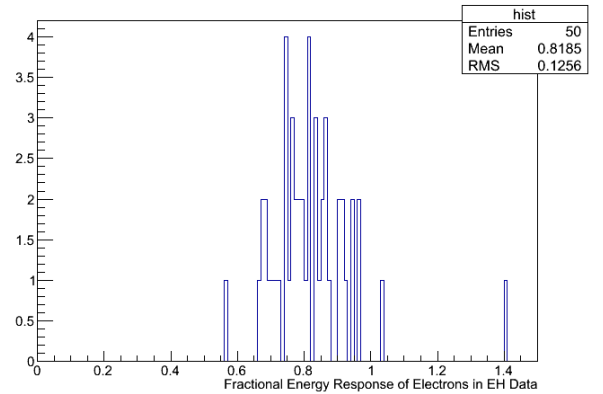


Figure 33: Histogram of electron calorimetric responses for electrons in ECAL-HCAL data.

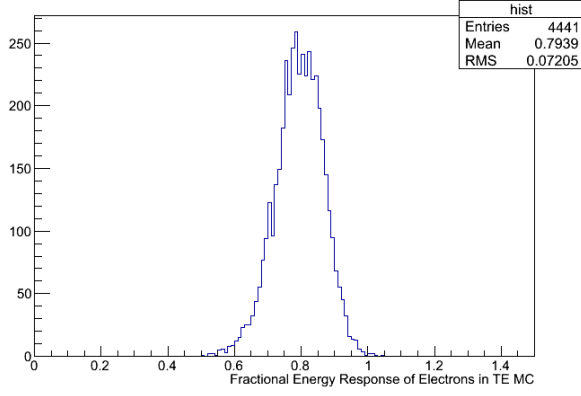


Figure 34: Histogram of electron calorimetric response for Tracker-ECAL MC.

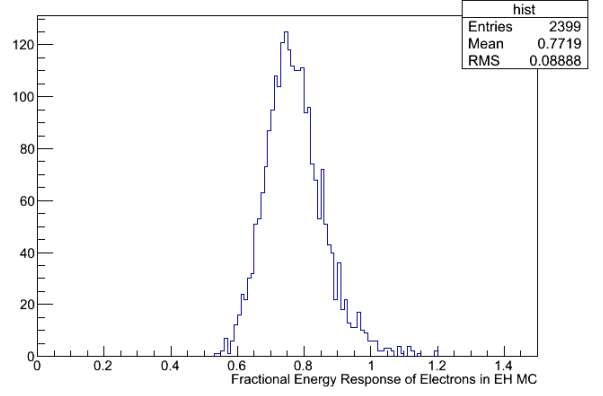


Figure 35: Histogram of electron calorimetric responses for electrons in ECAL-HCAL MC.

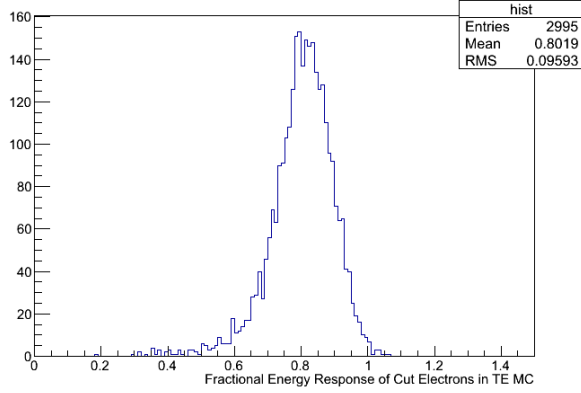


Figure 36: Histogram of calorimetric response for Tracker-ECAL MC electrons which do not fit the selection criteria.

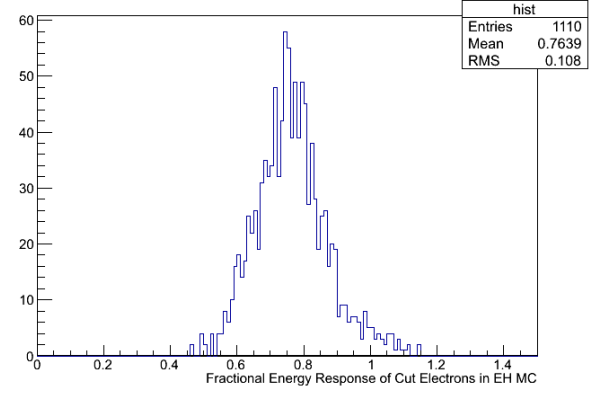


Figure 37: Histogram of calorimetric response for ECAL-HCAL MC electrons which do not fit the selection criteria.

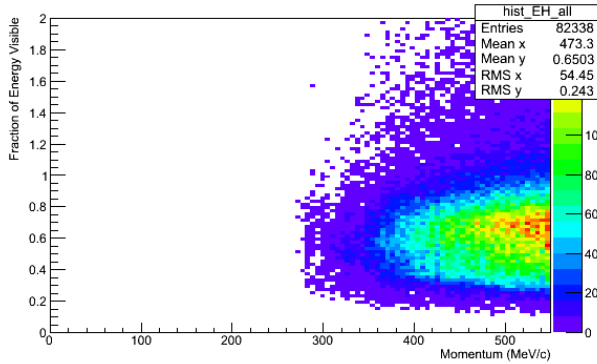


Figure 38: Calorimetric response as a function of momentum for pions and electrons in EH MC.

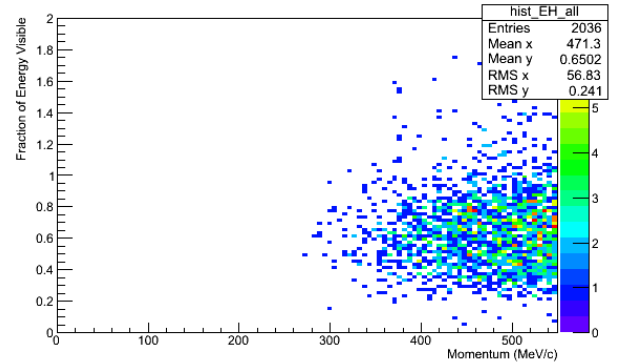


Figure 39: Calorimetric response as a function of momentum for pions and electrons in EH data.

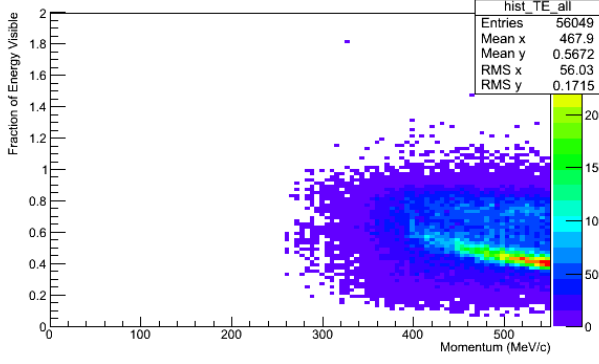


Figure 40: Calorimetric response as a function of momentum for pions and electrons in TE MC.

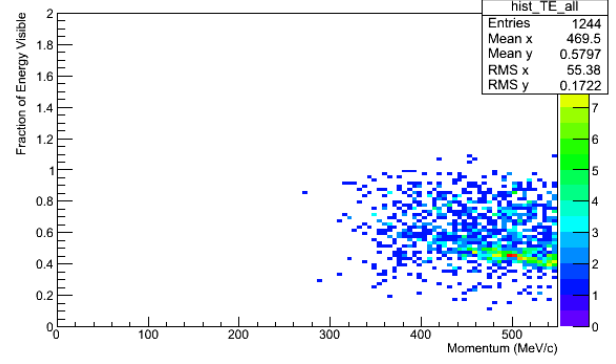


Figure 41: Calorimetric response as a function of momentum for pions and electrons in TE data.

Systematic Errors

Systematic	T/E e	E/H e	E/H pi-	E/H pi+	E/H e/pi-	E/H e/pi+
Cut events with over 1 Mev in last 4 planes	0.008	0.000	0.000	0.006	0.000	-0.006
Cut hits below 0.5 MeV	-0.012	-0.007	-0.021	-0.013	0.013	0.006
Cut hits in edges of U and V planes	0.001	-0.006	-0.002	-0.006	-0.004	0.000
Cut events with 5 or more related events	0.000	0.000	0.000	0.000	0.000	0.000
Cut events with another event within 800 ns	-0.001	0.001	0.006	0.006	-0.005	-0.004
Lower Birk's constant by 15% in MC	0.006	0.002	0.013	0.012	-0.009	-0.008
Raise Birk's constant by 15% in MC	-0.001	-0.003	-0.014	-0.012	0.010	0.009
Track node cut lowered 10%	-0.001	0.004	0.000	0.000	0.004	0.004
Track node cut raised 10%	0.000	0.001	0.000	0.000	0.001	0.001
Back-half cut lowered 10%	0.000	-0.001	0.000	0.000	-0.001	-0.001
Back-half cut raised 10%	0.000	0.001	0.000	0.000	0.001	0.001
Module variance cut (lower bound) lowered 10%	0.000	0.000	0.000	0.000	0.000	0.000
Module variance cut (lower bound) raised 10%	0.000	0.000	0.000	0.000	0.000	0.000
Number of raw hits cut lowered 10%	0.007	-0.007	0.000	0.000	-0.007	-0.007
Number of raw hits cut raised 10%	0.002	0.008	0.000	0.000	0.008	0.008
Time of flight cut raised to 20.72 ns	0.003	0.003	0.000	0.000	0.003	0.003
Time of flight cut lowered to 10.28 ns	0.004	-0.003	0.000	0.000	-0.003	-0.003
Tracker-ECAL upper bound on module variance lowered 10%	0.007	0.000	0.000	0.000	0.000	0.000
Tracker-ECAL upper bound on module variance raised 10%	0.000	0.000	0.000	0.000	0.000	0.000
Lead density lowered 2.4% in ECAL	0.003	0.007	0.001	-0.001	0.006	0.007
Lead density raised 2.4% in ECAL	-0.002	-0.004	-0.006	-0.009	0.002	0.005
Polystyrene density lowered 3.5%	N/A	N/A	N/A	N/A	0.003	0.009
Overall energy scale lowered 3%	-0.026	-0.028	-0.030	-0.030	N/A	N/A
Overall energy scale raised 3%	0.026	0.028	0.030	0.030	N/A	N/A
Use effective rest mass subtraction	0.000	0.000	0.000	0.000	0.000	0.000
Lower momentum 1%	0.008	0.009	0.011	0.010	-0.001	-0.001
Raise momentum 1%	-0.008	-0.007	-0.010	-0.011	0.002	0.003
PMT Nonlinearity	-0.002	-0.004	-0.009	-0.009	0.005	0.005
Total Systematics	0.032	0.032	0.042	0.039	0.021	0.020

Table 9: A list of the systematic errors on the e/π ratio. The specific errors are described in more detail below in the order in which they appear in the table. The signs denote the direction in which the value changed after applying the variation. When I have two cuts listed with the variation going in opposite directions, I averaged the changes and took that as the relevant systematic error.

7.3 Edges of U and V Planes

Out of fears that the edges of the U and V planes might be contaminated by particles which were not bent by the magnet, we cut hits in the U and V planes which were above strip 58 or below strip 8. See also docdb 9577.

7.4 Extra Time Slices

Based on Rik's work, we cut events with 5 or more time slices.

7.5 Nearby Time Slices

Based on Rik's work, we cut events with another event within 800 ns.

7.6 Birk's Constant

Based on Rik's work, we shifted Birk's constant up and down 15% in MC.

7.7 Electron Cuts

We varied our electron cuts up and down by 10%. This value was chosen as a rough estimate of my uncertainty in the optimal cutoff point. Based on information in docdb 5424 indicating a TOF error of 0.22 ns, we varied the time of flight cut from 20.5 ns to 20.28 ns and 20.72 ns.

7.8 Lead and Polystyrene Densities

We varied the lead density in the MC ECAL by 2.4% in both directions and the polystyrene density by 3.5% down. These were both 2 sigma variations, so the values shown in the table are halved. Since it was already accounted for elsewhere, we left the polystyrene values out of the calculation of our total systematic error except for the double ratios.

7.9 Overall Energy Scale

We varied the overall energy scale by increasing or decreasing the energy reconstructed in each hit in the Monte Carlo by 3%. This was done only for the single particle ratios, since it would cancel out for the double ratios.

7.10 Effective Rest Mass

Earlier, I had been using an effective mass subtraction to calculate the true energy, where I subtracted off 50 MeV from the true energy as an effective rest mass, based on Ronny's results in docdb 9016. I did not do this in the final version, but compared with what would have happened if I did as a systematic.

7.11 Momentum Change

Inspired by Rik's technote, we raised and lowered the momentum of MC particles in the beamline by 1%. This value was chosen based on the value Josh gives in docdb 8496.

7.12 PMT Nonlinearity

We looked at the hit_q distribution for electrons in the T/E and E/H in both data and Monte Carlo, then scaled them by a factor of $-0.000214286hitq^2 - 0.000142857hitq + 1.0$, where *hitq* is the deposited charge measured in pC, and saw how the means of the distributions changed. I took the error as half of this difference, using the data distribution. The above formula was given to me by Rik Gran. The results are shown in Tab. 10. The plots are shown as Fig. 42 - 49. I have done this systematic just for electrons, since Rik has found the pion error. See docdb 9999.

Nonlinearity Systematic Error

Configuration	Uncorrected Mean (fC)	Corrected Mean (fC)	Percent Change	Percent Error
T/E Data	936.9	933.1	0.41	0.20
E/H Data	996.7	988.6	0.81	0.41
T/E MC	740.9	738.2	0.36	0.18
E/H MC	793.6	788.7	0.62	0.31

Table 10: Percent error in the mean of the hit_q distribution due to PMT nonlinearity.

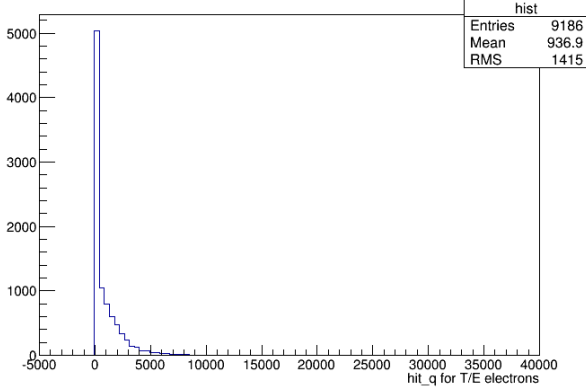


Figure 42: Distribution of hit_q (in fC) in T/E data before applying the PMT nonlinearity correction.

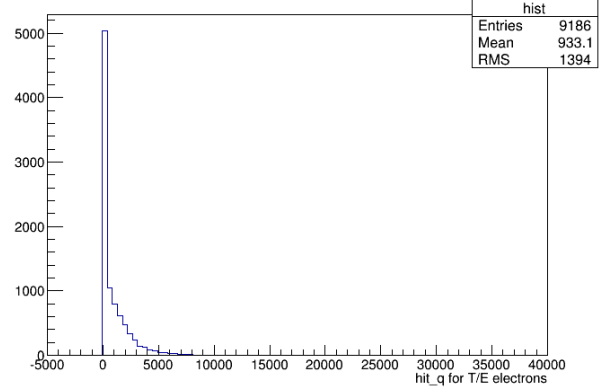


Figure 43: Distribution of hit_q (in fC) in T/E data after applying the PMT nonlinearity correction.

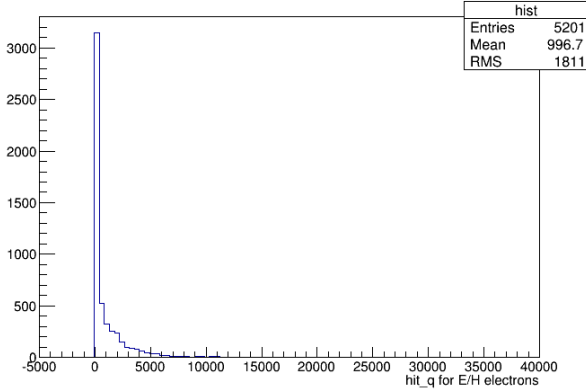


Figure 44: Distribution of hit_q (in fC) in E/H data before applying the PMT nonlinearity correction.

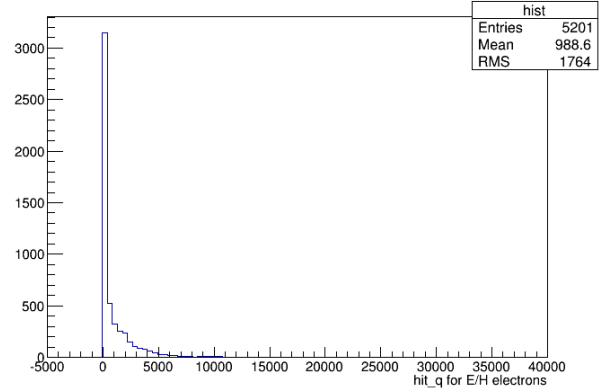


Figure 45: Distribution of hit_q (in fC) in E/H data after applying the PMT nonlinearity correction.

EH Summary Table

Particle	MC/Data
e	0.969 ± 0.017 statistical ± 0.032 systematic
π^- 450-550 MeV	1.017 ± 0.016 statistical ± 0.042 systematic
π^+ 450-550 MeV	0.996 ± 0.017 statistical ± 0.039 systematic
e/π^- 450-550 MeV	0.953 ± 0.022 statistical ± 0.021 systematic
e/π^+ 450-550 MeV	0.973 ± 0.023 statistical ± 0.020 systematic

Table 11: Summary of the MC/data results for EH electrons and pions.

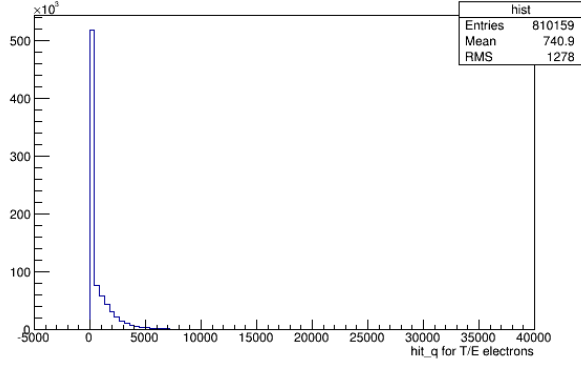


Figure 46: Distribution of hit_q (in fC) in T/E MC before applying the PMT nonlinearity correction.

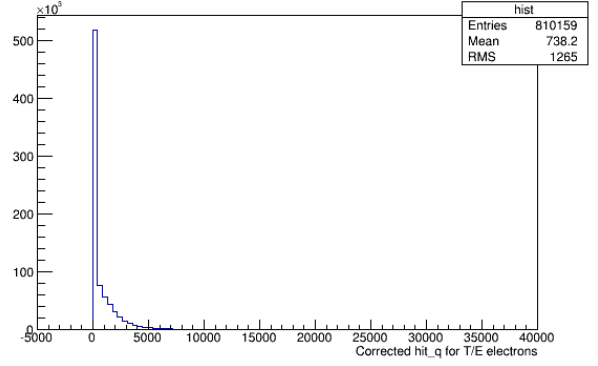


Figure 47: Distribution of hit_q (in fC) in T/E MC after applying the PMT nonlinearity correction.

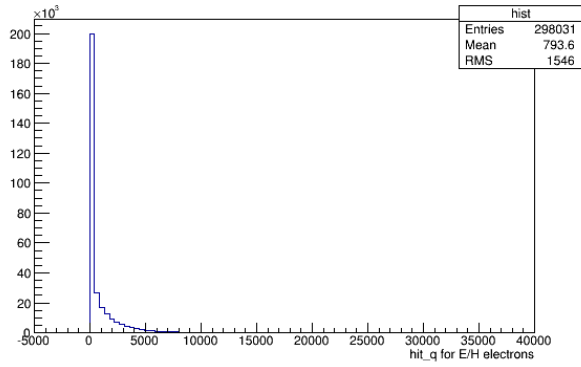


Figure 48: Distribution of hit_q (in fC) in E/H MC before applying the PMT nonlinearity correction.

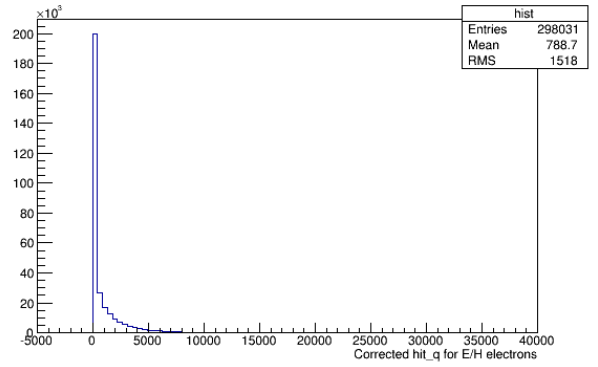


Figure 49: Distribution of hit_q (in fC) in E/H MC after applying the PMT nonlinearity correction.